Surface Science 273 (1992) 147–159
North-Holland

surface science

Spin polarization of secondary electrons from Fe(110) excited by unpolarized primary electrons

J. Kirschner

Freie Universität Berlin, Institut für Experimentalphysik, Arnimallee 14, D-1000 Berlin 33, Germany

and

K. Koike

Advanced Research Laboratory, Hitachi Ltd., Hatoyama, Saitama 350-01, Japan

Received 2 January 1992; accepted for publication 14 February 1992

We report on angle- and energy-resolved spectroscopy of secondary electrons from Fe(110). Intensity and polarization distributions in normal emission as a function of energy of the primary electrons are studied. For the first time angle-resolved spectra as a function of emission angle are measured and compared to theoretical calculations of the polarization fine structure. The influence of oxygen exposure on the polarization spectra is studied and surface-related features are identified. We conclude that surface resonances as well as the bulk band structure both contribute to the polarization fine structure. Consequences for the analysis of magnetic microstructures in a scanning electron microscope with polarization analysis are pointed out.

1. Introduction

The spin polarization of secondary electrons from ferromagnets was discovered in 1976 by Chrobok and Hofmann [1]. When bombarding a polycrystalline EuS film by unpolarized primary electrons, they observed up to 32% polarization, and found the vector orientation to be antiparallel to the magnetization. Since then, a number of studies have been carried out, partly motivated by the development of scanning electron microscopy with spin polarization analysis of the secondaries [2–4], since a fundamental understanding of the polarization properties is vital to its application [5]. Spin polarization properties of secondary electrons from the following bulk samples have been investigated: the metallic glasses $Fe_{81}B_{15}Si_4$ [6,7], $Fe_{60}Ni_{20}B_{20}$ and $Fe_{44}Ni_{37}B_{19}$ [7], $Fe_{83}B_{17}$ [8], poly-crystalline permalloy [9], Ni(110) [10], Co(1010) [11], and Fe(100) [11,12]. To date, a general qualitative understanding of the polarization spectra has been achieved, but for a quantitative understanding more data on well-defined clean single-crystal surfaces are required. The purpose of the present study is to provide angle-resolved data on the spin polarization and intensity distribution of secondaries from Fe(110) excited by unpolarized primary electrons of variable energy. Some part of this work has been presented previously [13], though without experimental details. These will be given in section 2. In section 3 results for normal emission and spin polarization spectra for off-normal emission are presented, followed by a discussion in section 4. A few conclusions related to the operation of a scanning electron microscope with spin polarization analysis are drawn in section 5.

2. Experimental aspects

For the experiments the analyzer part of the "complete scattering experiments" described earlier [14] was used, but in a different configuration

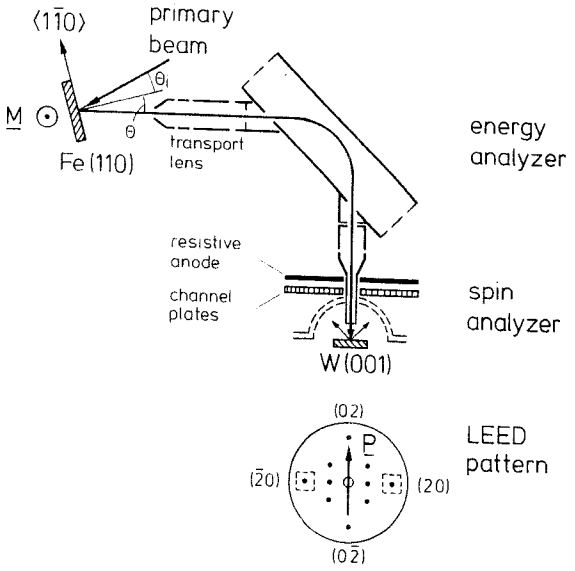

Fig. 1. Schematic view of the experimental apparatus for the angle-resolved measurement of intensity and polarization distributions of secondary electrons from Fe(110), excited by unpolarized primary electrons.

of the sample orientation and magnetization. As shown schematically in fig. 1, the apparatus consists of three main parts: the magnetized sample, the energy analyzer with transport lens, and the spin analyzer following the energy analyzer. The sample is a Fe(110) crystal, magnetized along the [100] direction, and held by a soft iron yoke. In the sketch of fig. 1 the magnetization points into or out of the paper plane. It was assured by in situ magnetic Kerr effect observation that the sample surface was in a single-domain state along the magnetization direction. The sample was extensively cleaned by heating and sputtering along established procedures [15,16], until heating above the Curie temperature did not result anymore in noticeable impurity segregation (mainly S). For its final preparation the target was sputtered by 2 keV Ar^+ ions to remove traces of oxygen. This leads to carbon enrichment at the surface due to preferential sputtering. The remaining C was removed by "titration" with oxygen (i.e. oxidation) at 550°C until the surface was found "Auger-clean". A very clear LEED pattern with strong contrast was observed as a result. Since we found that the spin polarization signal itself is somewhat more sensitive to contamination than Auger spectroscopy, the polarization served as the final check. The secondary electrons were excited by a glancing incidence gun located above the paper plane at an angle of 50° with respect to the axis of the transport lens. The take-off angle θ was varied by rotating the sample, which caused the angle of incidence with respect to the surface normal, θ_i, to vary between 45° and 55°. The transport lens consists of 5 cylindrical electrodes and accelerates or decelerates the electrons into the electrostatic analyzer, working at a constant pass energy. The geometrical angular resolution given by the aperture size and its distance to the sample is about ±3°. When the sample was biased with respect to ground by −10 V, which was necessary for obtaining the data in figs. 2 and 3, the effective acceptance angle for the very-low-energy electrons may increase to ±5%. The electrostatic analyzer is of the cylindrical mirror type, operating in second-order focusing at 90° deflection angle. With its constant pass energy set at 12 eV the energy resolution was about 0.3 eV, as may also be read from the low-energy edge of the intensity distribution curves in fig. 2a. After energy analysis the electrons are accelerated to an energy of 104.5 eV, and focussed into the LEED-type spin analyzer [17]. The elastically diffracted electrons from the W(001) surface (secondaries are suppressed by the hemispherical grids) are multiplied by a two-stage channelplate amplifier and detected by a position sensitive readout using a resistive anode. After a short integration time a "LEED pattern" (as indicated in fig. 1) may be observed on an oscilloscope storage screen. The relative count rate difference of the pair of ⟨20⟩ beams, which is obtained by setting electronic windows around the corresponding diffraction spots, yields a measure of the sign and magnitude of the spin polarization vector $\boldsymbol{P}$ normal to the paper plane. The corresponding ⟨02⟩ pair measures a horizontal component, which was found to be zero, as was expected, since the magnetization was normal to the paper plane. Since the emission plane coincides with a (100) mirror plane of the crystal, any polarization component due to spin–orbit interaction in the sample is also along the normal to

the paper plane [17]. This contribution was removed by measuring the secondary electron spin polarization for opposite magnetizations and taking the difference. In a previous "worst case" experiment it has been shown that the polarization vector and the magnetization vector are parallel to within the experimental accuracy of $\pm 1.5°$ [18]. Since the present geometry is more symmetric than that in ref. [18], we can make sure that the full polarization vector is measured.

3. Results

In the first place we used the normal-emission geometry, since this is the preferred geometry for scanning electron microscopy with spin polarization analysis. We are interested in the evolution of the intensity and spin polarization distributions as a function of the primary energy. Similar data have been measured previously for polycrystalline [2] or amorphous material [8] but not for a single crystal in an angle-resolved experiment. In order to discriminate secondaries from the chamber wall and lenses, excited by backscattered electrons, we biased the sample -10 V negative with respect to ground. This caused no significant change of the polarization distributions, though the effective solid angle becomes slightly energy dependent. Its effect on the intensity distribution as well as that of a slightly energy-dependent transmission of the transport lens was not corrected, since we are interested in relative changes of the intensity distribution curves. Fig. 2a shows the measured intensity distribution curves for different primary energies, while fig. 2b shows the polarization distribution curves for similar energies. The intensity distributions show the well-known behaviour with a pronounced peak at low energy and a gradual decrease towards higher kinetic energy. A slight hump between 15 and 20 eV is visible at all primary energies, though the slope of the distribution changes. We note that the shape of the distributions stabilizes beyond a certain primary energy. This is seen by comparing the distributions for 490 and 1990 eV primary energy. Except for a barely visible increase at very low energies, the 1990 eV curve has the

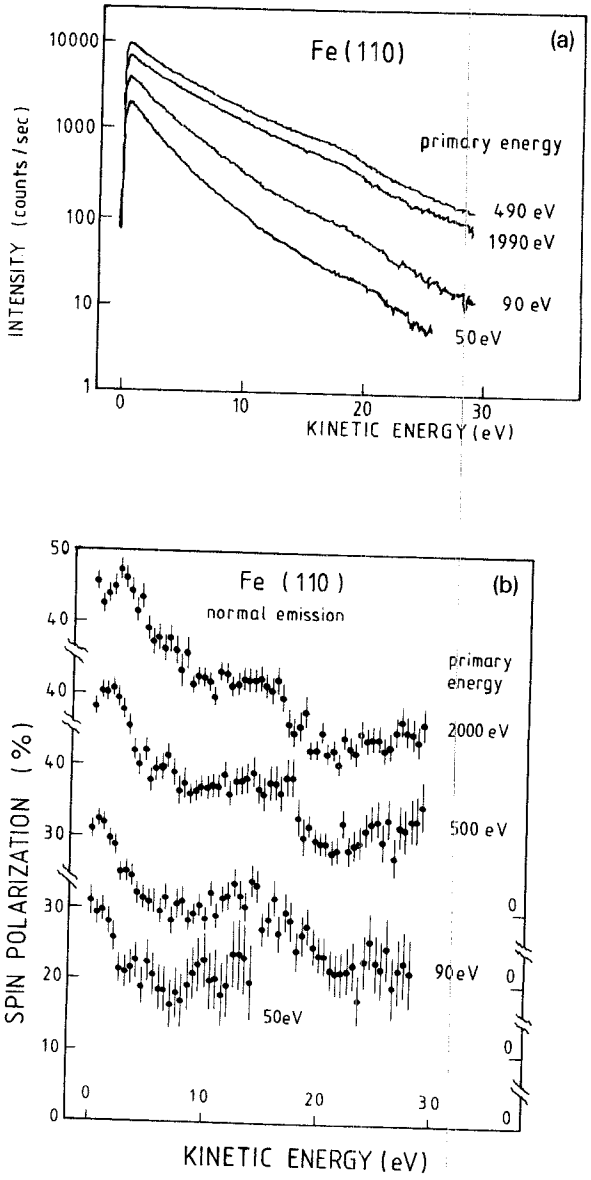

Fig. 2 (a) Intensity distribution curves for secondary electrons from clean Fe(110), emitted around the surface normal, with the primary energy as a parameter. The angle of incidence, θ_i, is $\sim 50°$ with respect to the surface normal. The count rate is normalized to constant primary beam current. Note that the distribution curves for 490 and 1990 eV have the same shape, except for a minute enhancement at very low energy. (b) Spin polarization distribution curves for the same conditions as in (a). The vertical bars give the 1σ-statistical error. Note that the "plus/minus" feature around 15–20 eV is associated with a hump in the intensity distribution curves around the same energy.

same shape as that at 490 eV primary energy, but is scaled down by a certain factor.

Turning to the polarization distributions, we note that the polarization at low kinetic energy increases with the primary energy from about 30% at 50 eV to almost 50% at 2 keV. We also notice a pronounced "plus/minus" polarization feature in the range of 15 to 20 eV which is obviously related to the intensity hump in fig. 2a. By shifting the polarization distributions such that they lie one on top of the other, we found that this plus/minus feature is, within the statistics, the same at all energies: in particular does its amplitude *not* increase with increasing primary energy. This rules out the possibility of this feature being a low-energy portion of the multiplet Coster–Kronig-type Auger transition near 45 eV, since its intensity should drastically diminish when the primary energy approaches its excitation threshold. This observation, together with the dispersion properties of this feature to be shown below, prove that the fine structure on the polarization distributions is due to the crystallinity of the sample. While the fine structure is very similar in all distribution curves, there is a noticeable exception near 2 eV (the data points have been taken in 0.5 eV intervals): with increasing primary energy an additional fine structure peak evolves around 2 eV which remains constant above about 1 keV primary energy. With this exception, our observations lend further support to the assumption of Tamura and Feder [19] that the polarization distribution is additively composed of a smooth "cascade"-related function, which may depend on the primary energy, and an energy-independent fine structure due to the bulk band structure of the crystal.

To check this point further, and in order to make contact with standard measurements of secondary electron emission, we measured the total secondary electron yield as a function of primary energy, together with the polarization at several secondary energies. The geometrical conditions are the same as in fig. 2. The results are shown in fig. 3, where the total secondary electron yield is plotted on the left hand scale, while the natural logarithm of the ratio of majority spins $N_\uparrow$ to minority spins $N_\downarrow$ is plotted on the right-hand

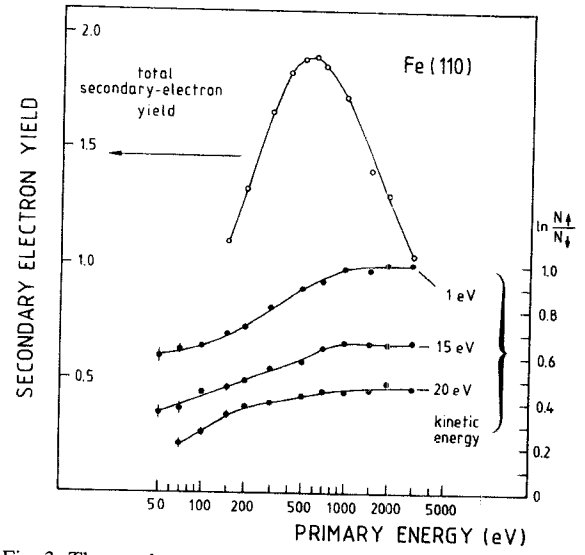

Fig. 3. The total secondary electron yield from clean Fe(110) (left-hand scale) versus the primary beam energy. The logarithm of the ratio of majority electrons $N_\uparrow$ and minority electrons $N_\downarrow$ is plotted on the right-hand scale for 1, 15, and 20 eV kinetic energy of the secondary electrons. The angle of incidence is $\sim 50°$ with respect to the surface normal. The polarization data refer to normal emission within a solid angle of $\gtrsim \pm 5°$. Note that the saturation of the polarization is reached beyond the energy where the maximum total yield is reached.

side. The secondary yield was determined at each energy by varying the bias potential in the range -50 to $+50$ V while recording the target current. The yield was determined from the asymptotes and the measured value at zero bias in the usual way. The accuracy of this procedure is not as good as that of more sophisticated collector methods [20], but the relative accuracy is adequate for our present purpose of relating the total yield curve with polarization data. This method is limited to the condition of the primary energy being large compared with the bias potential. Therefore we discarded the data below 150 eV primary energy where this condition was not met, even for smaller bias potential scans. For the total yield we observe the usual curve [20] with a maximum of the yield around 500 to 600 eV and a drop on both sides. We note that the variation of the total yield with energy is consistent with the relative areas under the intensity distribution

curves in fig. 2a, which have been observed in normal emission.

It is obvious from the polarization spectra in fig. 2b, that the spin polarization of the secondary electrons also depends on the primary energy. It is not clear, however, whether the polarization increases uniformly by a certain scaling factor upon increasing the primary energy, or whether the spectral distribution changes its shape. Therefore, we measured the polarization at selected kinetic energies of 1, 15, and 20 eV for a wide range of primary energies, and plotted them in fig. 3 on a logarithmic scale. The ratio of majority to minority electrons, plotted on the right hand scale, is related to the polarization P by

$$\ln(N_\uparrow/N_\downarrow) = \ln[(1+P)/(1-P)]$$
$$= 2(P + P^3/3 + P^5/5 + \cdots).$$

We plotted the polarization data in this way since the logarithmic scale allows to compare the *shape* of the curves in a direct way. If they had the same shape at all secondary kinetic energies, but were scaled by a certain factor only, they would just appear shifted with respect to each other in fig. 3. Evidently, there is no such scaling factor and the shape of the curves is different. Though for all three energies the polarization is higher at a high primary energy than at a low energy, the relative increase in polarization with increasing primary energy is much larger at 1 eV than at 20 eV.

The data points for 15 and 20 eV kinetic energy at low primary energy deserve further comment: at low primary energy, and if the secondary electron energy is not very small compared to the primary energy, the measured polarization is not that of the secondary electrons only [18]. Since the secondary electron yield is low, a fraction of inelastically scattered primary electrons, which are unpolarized, at the same kinetic energy tends to diminish the polarization. For this reason we consider these data points as not representing the true secondary electrons' polarization.

Comparing the polarization data to the secondary electron yield curve we note that the saturation of the polarization occurs close to, but *beyond* the primary energy where the maximum yield is observed. This important finding, bearing on the mechanism of the generation of spin-polarized electrons in the collision cascade, will be discussed in section 4. We note here that qualitatively very similar results have been obtained on bulk Fe(100) by Paul et al. [21]. They also show the polarization to saturate beyond the energy of the maximum yield, and also find the polarization enhancement to be stronger for low-energy secondaries than for high-energy ones. The second part of our experiments concerns the polarization fine structure superimposed onto the smooth "cascade polarization". Taborelli [22] compared in unpublished work the polarization spectra from Fe(100) and Fe(110) in normal emission and showed that at oblique emission from Fe(100) the spectrum of the (110) surface is obtained in good approximation at an emission angle of 50°, i.e., approximately along the [110] direction. Our results for normal emission from Fe(110) are in good qualitative agreement with that of Taborelli, though the magnitude of polarization is higher by about a factor of 1.2 in our case. The reason(s) for this discrepancy are not yet known.

We studied the evolution of the polarization spectra for various take-off angles from Fe(110) and compare them to calculated fine structures in section 4. For these measurements we used a primary energy of 2.5 keV, i.e., well in the saturation regime, and a sample bias potential of 0 V to remove the distortion of the trajectories. The results for take-off angles from $\theta = 0°$ to $\theta = 60°$ are shown in fig. 4. We observe that the maximum polarization near zero energy is similarly high in all cases, followed by a gradual decrease towards higher kinetic energy. We note also a strong dependence of the fine structure on the emission angle and dispersive behaviour (e.g., for $\theta = 0°$ and $\theta = 15°$ around 10 eV). This demonstrates unequivocally that the fine structure is due to the crystallinity of the sample. By averaging over all emission angles, such as in a microscope, these features tend to average out. Our attempt to recover the presumably smooth "cascade" polarization function by averaging over the available angle-resolved data was not quite successful, though. The averaged data do indeed

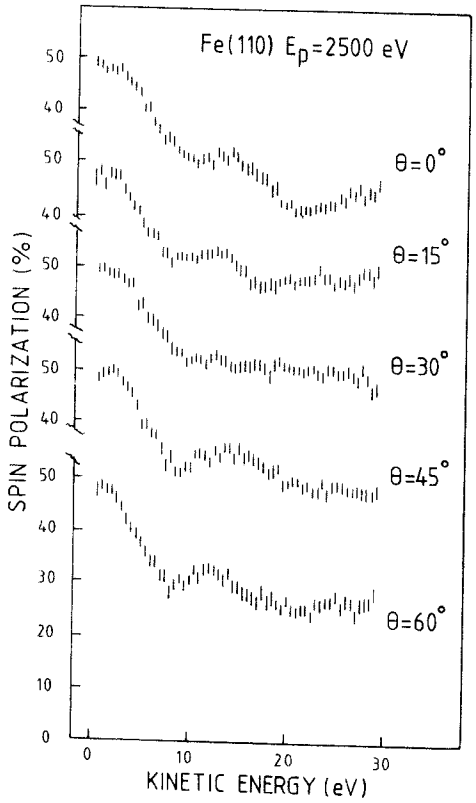

Fig. 4. Angle-resolved secondary electron spin polarization distributions from clean Fe(110), with the take-off angle θ relative to the surface normal as a parameter. The vertical extension of the bars indicates the $\pm 1\sigma$ statistical error. Note the vertical shift of the curves by 20% each.

show a much smoother behaviour, but the pronounced minimum feature around 9 eV persists. The almost featureless curve for $\theta = 30°$ turned out not to be well suited to describe the "background" since it often lies above the other curves. Thus, it appears that the determination of the cascade polarization is not an easy task, at least not with single crystals. Therefore, we tried to simulate "amorphous Fe" by sputtering the surface extensively by various noble gas ions with different energies. These attempts, however, failed for two reasons: first, we never were able to destroy the long-range crystalline order completely according to the LEED pattern, which still showed diffractions spots, though diffuse. Second, preferential sputtering was always present and led to carbon enrichment at the surface. Since the polarization data from such a surface cannot reliably be compared with those from a clean surface, we tried to "titrate" the carbon away by oxygen exposure. This necessarily involved heating above 450°C, after which a clear, sharp LEED pattern reappeared. We conclude that the polarization of the cascade contributions remains unknown, at present.

It is well known that the fine structure in secondary electron intensity spectra reflects both bulk- and surface-related features [23–26]. For the polarization fine structure this question has

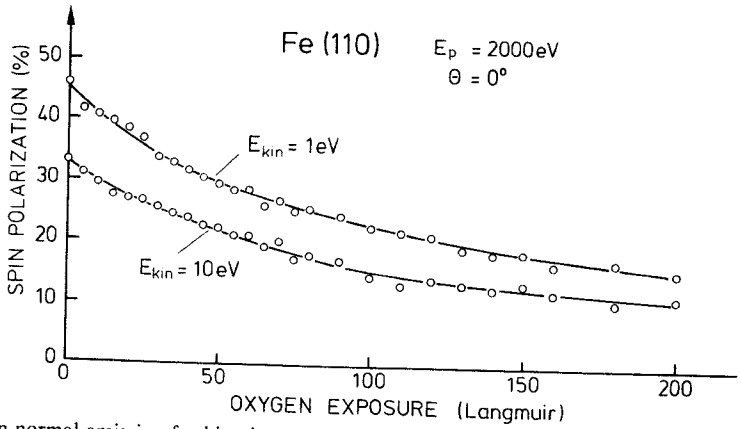

Fig. 5. Spin polarization in normal emission for kinetic energies of 1 and 10 eV as a function of exposure to oxygen. The decay rate is faster for small kinetic energy than for the larger one.

not been treated yet. So far, the fine structure has been traced back to the *bulk* band structure above the vacuum level [19]. The standard experimental tool to distinguish between bulk- and surface-related features is to absorb reactive gases at the surface. Though this is not an unequivocal proof of surface effects under all circumstances, this technique usually gives a good hint. For this reason we studied the behaviour of the secondary electron polarization upon exposing the surface to increasing doses of oxygen at room temperature. Fig. 5 shows the spin polarization at two kinetic energies (1 and 10 eV) at normal emission as a function of oxygen exposure up to 200 L. As expected, we find a gradual decrease at both energies since the oxide formation leads to a decrease of the magnetic moment at the surface. These data are also relevant for applications of the scanning electron microscope with polarization analysis since they show in a quantitative way the effects of oxygen contamination on the magnetic contrast. A closer inspection shows in addition, that the polarization at 1 eV kinetic energy drops *faster* with increasing oxygen exposure that at 10 eV. Plotting the data in form of $\ln(N_\uparrow/N_\downarrow)$ like in fig. 3 confirmed that there is not a common scaling factor between the two curves. A similar study was carried out on Ni(110) [27] with different results. There, a faster initial decrease, followed by a plateau up to 2 L and a slower decrease to 50 L was observed. Much less difference for electrons with 0 and 10 eV kinetic energy was found. We attribute the more gradual decrease with Fe(110) to the different characteristics of oxygen uptake and oxide formation. The faster decrease at low kinetic energy has its origin in a change of shape of the polarization distribution. This is seen in fig. 6, where we compare the polarization spectrum from the clean surface to that from the surface exposed to 50 L oxygen (corresponding to about 1 ML coverage) for the same experimental conditions. Clearly, the decrease at 30 eV is much less than at low energies. Evidently, the peak around 2 eV vanishes, while the features around 20 eV persist. This leads us to the conjecture, that the latter feature is related to the bulk bandstructure while the low-energy features are at least in part related to the surface

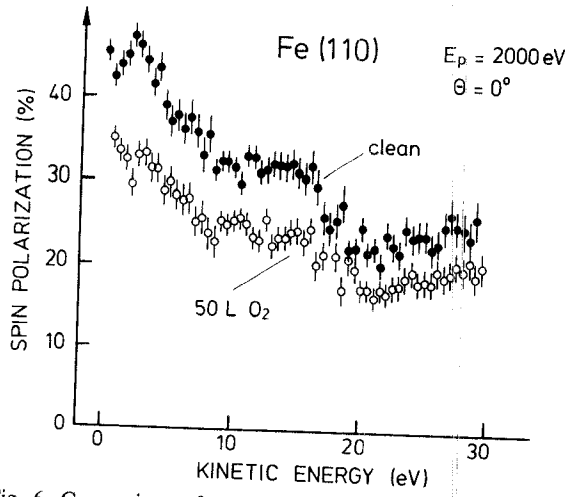

Fig. 6. Comparison of secondary electron spin polarization spectra from the clean surface and after exposure to 50 langmuir O_2. Note that the surface peak at ~2 eV disappeared while the bulk-related features around 20 eV are much less affected.

electronic structure. This will be discussed in more detail below.

4. Discussion

Our discussion of the preceding results will focus on the following questions: how can the polarization enhancement at low energies and its dependence on the primary energy be understood, and what is the role of surface electronic states in this process? We first make reference to established models of the secondary electron generation process, which have been developed some decades ago. A source of references may be found in Seiler's review [20].

The shape of the total yield curve, cf. fig. 3, is explained in the following way: starting from low primary energies more and more energy is dissipated by the primary electrons in plasmon excitation, electron–hole pair production and, when the energy suffices, in core-level ionization. Inelastically scattered primary electrons may dissipate energy in smaller and larger portions until they come to rest, predominantly inside the solid. On their way they may have created some high-

energy secondaries, which in turn produce tertiary electrons and so on, up to higher generations. This process resembles a collision cascade in ion–solid interaction and the secondaries are said to be generated in a cascade process involving many generations of secondaries. With increasing primary energy more and more secondaries are generated in total, but also the relative number of high-energy secondaries increases, as may be seen in the intensity distributions of fig. 2a. Simultaneously with the increase of the amount of energy deposited in the solid, the center of gravity of the region where the cascade develops moves to larger depth, since the projected range of the primary electrons increases with energy. (At a few keV energy the projected range of the primaries is of the order of several 100 nm to several 1000 nm for medium to light weight materials.) Since the secondaries also dissipate energy on their way to the surface, they have the less chance to overcome the surface barrier, the deeper inside they have been generated. Thus, there exists a certain primary energy, usually of order several 100 eV to 1 keV, where a maximum of the yield is obtained. Beyond this energy, in total more secondaries are generated inside the material, but this occurs at such large a depth that only a small part of them arrives at the surface with sufficient residual energy to overcome the surface barrier. At the energy of the maximum yield, and beyond, the intensity distribution curves become essentially stationary (see fig. 2a) but the overall yield decreases. Only at the very low energies a slight increase may be found as has, e.g., been observed by Palmberg [28] on clean Ge, and also in the present work, though barely visible on a logarithmic scale. These are electrons that come from deep below the surface, having dissipated their energy in many inelastic collision events. They barely overcome the surface barrier, possibly only after several reflections between the surface barrier and the top atomic layer.

How is this picture related to the energy dependence of the polarization enhancement, e.g., the curve for 1 eV kinetic energy in fig. 3? It has been commonly accepted that among various energy loss mechanisms Stoner excitations [10,11, 13,14,29,30] play a major role for the secondary electron polarization from ferromagnets. Stoner excitations are characterized by an electron of a particular spin state above the Fermi level, coupled to a hole in a band of opposite spin character below E_F. These electron–hole pairs may be generated by a two-electron exchange scattering process in the following way. Assume a secondary electron, e.g., with energy $E_S = 20$ eV above the Fermi energy, and having minority spin character, to scatter with a majority-type electron below E_F. After the elastic scattering event the minority electron must have found an empty state above E_F, while the majority electron is raised up in energy, almost to the level which the minority electron had before scattering. The difference in energy is the energetic difference between the state now occupied by the minority electron (above E_F) and the state previously occupied by the majority electron (below E_F). This energy difference is typically of the order of the exchange splitting Δ of the spin-split bands in the ferromagnet, e.g., $\Delta \approx 2$ eV for Fe. As a result of this process we have another secondary electron with energy $E_S - \Delta$ and of opposite (= majority) spin character. The whole process looks *as if* we had an inelastic process with energy loss Δ and an *apparent* spin flip of the electron. (We emphasize, that in reality the electron–electron scattering is elastic and that the individual electrons preserve their spin orientation.) The interaction channel we described is, of course, only one among others; for example, there might be an exchange of electrons with the same spin (which would be indistinguishable from a direct scattering process), or there might be a majority-type secondary electron "converted" into a minority-type one. "Complete" electron scattering experiments [14,30] proved that the exchange processes leading to an apparent spin flip contribute about one third to one half to the total intensity at the typical energy loss Δ. These exchange processes therefore are by no means rare events, and we emphasize that they occur in "ordinary", i.e. paramagnetic, materials without exchange splitting as well – only the distinction between majority and minority electrons is senseless in this case.

For our present topic there are two additional

important aspects: (i) in a ferromagnet there are by definition more majority electrons (and more minority empty states above E_F) than minority electrons (and majority empty states above E_F). Therefore the process outlined above will on average occur more frequently than the opposite one, which means that the secondary electrons will be "enriched" in majority spin. (ii) The (apparent) spin reversal of a secondary electron is accompanied by an (apparent) energy loss of order Δ. As a consequence, if we take a certain kinetic energy E_S where we observe a certain majority spin polarization, we will at a lower energy $(E_S - \Delta)$ always find a higher spin polarization of majority character. This explains why even at low primary energies in fig. 3 we find higher polarization at 1 eV secondary kinetic energy than at 15 eV. This argument explains qualitatively the tendency of increasing spin polarization with decreasing kinetic energy. Attempts to cast this picture into a formal theory have been undertaken by Penn and coworkers [31,32] using the concept of a spin-dependent inelastic mean free path. This concept recently seemed to be corrobated by measurements on the attenuation length of low-energy electrons through a magnetic film [33] and its spin dependence, which was interpreted in terms of spin-dependent inelastic mean free paths. Very soon, however, it was shown by theoretical calculations that the attenuation could also be obtained by purely elastic spin-dependent scattering in the overlayer [34]. In spite of partly encouraging agreement between measured cascade polarization and calculated enhancement factors, the concept of spin-dependent mean free paths appears to be unsettled. In particular, the increase of the secondary electron spin polarization with increasing primary energy and its final saturation cannot be explained by spin-dependent inelastic mean free paths. For this the spatial evolution of the cascade with increasing primary energy has to be considered. As mentioned above, at low primary energy the cascade is rather shallow and not fully developed. This means that many secondaries may escape the solid without major energy loss, in particular without having undergone exchange scattering processes. With increasing primary energy the cascade moves deeper into the solid, so that the secondaries observed outside have travelled increasingly longer path lengths. This means that the probability of exchange scattering with spin flip increases, as well as that of plural exchange scattering events. Since these events are accompanied by an energy loss, the relative increase of the low-energy secondaries is larger than that of the high-energy ones, enhanced by the energy dependence of the exchange scattering cross section. By tendency, the cross section is higher at low energies, but not much is yet known quantitatively for the exchange scattering with conduction band electrons in ferromagnets. Some results concerning the depolarization in inelastic scattering from a nonmagnetic system (Mo(110)) have recently been published by Mulhollan et al. [35] for the primary energy range from 10 to 90 eV. The results are in agreement with this expectation, showing larger depolarization at low primary energy than at higher energies. Since not all of the depolarization effect can be attributed to exchange processes (spin–orbit depolarization is significant in 4d metals), it seems unlikely that the exchange scattering cross section in ferromagnets changes drastically within several tens of eV, so as to cause a major contribution to the polarization enhancement at low kinetic energies.

The observation of polarization saturation of very slow secondaries near but beyond the energy of the maximum yield has also been made for thin iron overlayers (2 monolayers) on Au(100) by Paul et al. [21]. In this case the shape of the yield curve versus primary energy and the energy of maximum yield are determined by the substrate rather than by the overlayer and consequently are different from those of bulk Fe(100). The magnitude of the maximum polarization is much less than for bulk Fe ($\sim \frac{1}{4}$ of the bulk value for 2 ML Fe) since the secondaries arriving at the cover layer from below are unpolarized. Their energy distribution remains stationary upon increasing the primary energy, once the energy of the maximum yield is passed, and consequently the polarization of the secondaries remains constant. This picture is valid as long as the overlayer thickness is small compared to the maximum escape depth

of the secondaries (which depends on the substrate material).

The maximum escape depth of the secondaries is reached when the intensity distribution curves become stationary, i.e., near but beyond the maximum of the yield. Any further increase of the primary energy shifts the center of the collision cascade further inside, but the electrons that finally escape with minimum energy come from a certain maximum depth only (roughly 2 nm [20]). These electrons have had maximum probability to undergo spin flip scattering events and thus saturation is obtained. (One should keep in mind that 50% spin polarization means that three out of four electrons have their spin oriented along the same direction.) Complete spin polarization cannot be obtained since there are other, spin-independent energy loss mechanisms. As these are at least as important as the flip processes, the secondaries will be slowed down below the vacuum level before reaching their maximum polarization. However, the saturation value will depend on the existence and energy density of empty majority states above E_F since these enable the reverse spin flip scattering process, leading to an enrichment in minority-type secondary electrons. This argument may explain why the *relative* enhancement in Ni [10] is higher than in Fe: Fe has considerably more empty majority-type density of states than Ni. We note that the above explanation of the saturation of the spin polarization at a high primary energy is different from a previous explanation of a similar feature observed with $Fe_{83}B_{17}$ [8] and polycrystalline permalloy [9].

Turning to the polarization fine structure, we recall our observation in section 3, fig. 2 of the amplitude of the bulk-related fine structures being independent of the primary energy. This is in line with the fine structure of the intensity distributions being observable from rather low primary energies on. Obviously, the bulk states are populated, once the energy suffices. They may as well be populated by inelastically scattered primaries as they are by true secondaries. The spin polarization of the electrons emitted out of these states is determined by the spin character of these bands, rather than by inelastic scattering processes involving the spin-split density of states around the Fermi level. The escape depth of these electrons is determined by the usual inelastic attenuation length which is probably shorter than believed so far, not withstanding its possible spin dependence [33,34]. Since this is well within the projected range of primary electrons even of low energy ($\gtrsim 50$ eV) the bulk band states are populated even when the collision cascade has not fully developed. A possible higher population of these states due to a larger supply of electrons at higher primary energy may enhance the emission intensity somewhat, but not the spin polarization.

Within the surface-related fine structure at 2 eV kinetic energy we observed a polarization feature growing with the full development of the collision cascade. The growth of this feature correlates with an intensity increase at very low energy when the primary energy is at and beyond the energy of the maximum yield. Since the energy of these electrons matches well that of the surface state or surface resonance, we speculate that these are populated particularly easily, in the sense of a resonance phenomenon, by the very-low-energy secondaries when they arrive at the surface and possibly are multiply reflected by the surface barrier. We noted that these features are removed by oxygen exposure, while the bulk-related features essentially persist. These conjectures, based on experimental observations only, are corroborated by recent calculations by Tamura and Feder. Since these results will be published elsewhere [36], only a few essential points will be described here. The calculations were performed along the lines of the work by Tamura and Feder [19] for Fe(110) with two major additions: (i) for the first time calculations were done for a series of take-off angles from 0° to 60°, and (ii) the effects of the surface barrier on the polarization fine structure were studied in detail. Some results are shown in fig. 7, showing the polarization fine structure only, without the contribution from the secondary electron cascade. Two models for the surface barrier have been used: full multiple scattering between substrate and barrier, denoted by full lines in fig. 7, and restricted (2 times) multiple scattering (dashed lines). The former is appropriate for an

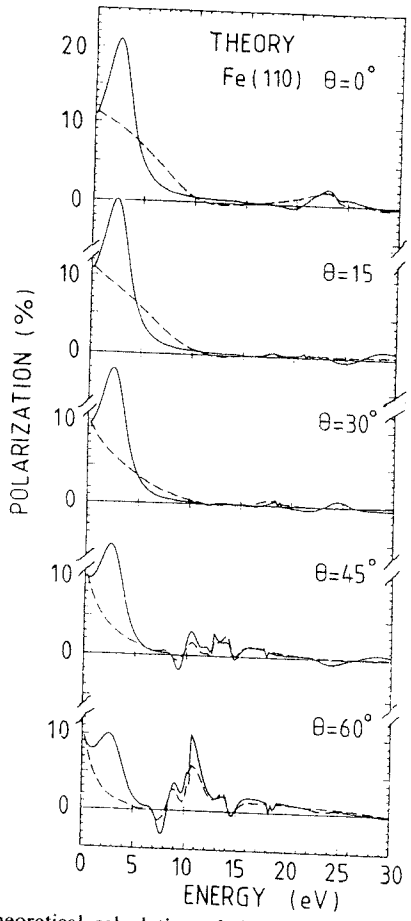

Fig. 7. Theoretical calculation of the spin polarization fine structure for the same angles as in the experiment. The full and dashed lines, respectively, denote a surface barrier model with full multiple scattering (solid lines) or reduced multiple scattering (dashed lines). The large peak around 2 eV obviously is a surface resonance, which is also observed experimentally (cf. fig. 6).

ideal rigid surface without defects and steps since it fully describes threshold resonances due to multiple scattering. A real surface shows defects and enhanced lattice vibrations which tend to destroy the phase relation between multiply scattered waves. In the calculations the influence of the surface may therefore be simulated by restricting artificially the number of multiple scattering events between substrate and surface barrier. Features which respond sensitively to this manipulation may be identified with surface resonances or, more generally, with surface-induced resonance structures. As shown by fig. 7, the latter barrier model tends to wash out resonance features over the whole energy range, but its effects are relatively small above 5 eV. A drastic effect is found around 2 eV, where the full multiple scattering model produces a large asymmetry peak of the majority type. This peak is very sensitive to the barrier model and may thus be identified with a surface-induced resonance feature. At small take-off angles the surface resonance dominates the asymmetry spectrum, while it is comparable to bulk features at larger angles. Comparing these results to the experimental data of fig. 4, we observe rather good general agreement at large angles, but less agreement at small angles, where the experimental structures are stronger than in theory. In any case, however, we find a rather strong polarization feature around 2 eV on the clean surface. Upon oxygen exposure this feature is strongly quenched at a coverage of ~ 1 ML. It is interesting to note that on Fe(100) a similar low-energy polarization feature was observed by Allenspach et al. [37] which also disappeared at a coverage of ~ 1 ML of oxygen (the exposures are different in both cases since the reactivity of both surfaces are different).

Thus, both theory and experiment lead to the conclusion that the fine structure in secondary electron polarization spectra is determined by the bulk band structure as well as by surface resonances. They seem to contribute by about equal amounts at a clean surface, while the bulk-related features survive at a slightly contaminated or otherwise disturbed surface.

5. Conclusions related to magnetic surface structure analysis

In the following some remarks shall be made which refer to the operation of a scanning electron microscope with spin polarization analysis of the secondary electrons.

(1) The polarization fine structure generally will be of minor importance since the angular integration by using polycrystalline material or an extraction field largely washes out this structure.

The structure due to surface states or surface resonances may contribute contrast effects on slightly but inhomogeneously contaminated surfaces.

(2) The choice of appropriate operating conditions for the primary beam source may be read from fig. 3. Since for SEM observations the very-low-energy secondaries are by far the most important ones (they are most easily collected and carry the largest spin polarization), the polarization curve for 1 eV kinetic energy and the yield curve are the most important data. The signal-to-noise ratio in a "magnetic map" is determined by the spin polarization times the square root of the secondary electron yield. Therefore, the microscope will preferably be operated in the regime of saturated polarization, which is beyond the energy E_m of the maximum yield. This energy depends on the material, the angle of incidence, and some other parameters [20]. The yield at a given energy beyond E_m may be increased by increasing the angle of incidence, but the distortion of the image soon limits this approach. Since the preferred take-off is normal to the surface for optimum collection efficiency, the geometry adopted in fig. 3 is thought to be close to the optimum. Thus, we arrive at the conclusion that an optimum signal-to-noise ratio will be obtained at a primary energy between 1 and 2 keV. With ordinary SEM columns the resolution at these low energies is rather poor, which strongly suggests the use of field emission cathodes for this purpose.

(3) The depth of magnetic information under these conditions is given by the escape depth of the secondary electrons. Contrary to many propositions [6,8,27,38–40] the escape depth is not given by the usual attenuation length λ (also sometimes called the "universal curve") but rather by an escape depth Λ which has to be used in the presence of a continuously slowing down process, and in the presence of a high-energy filter, represented by the surface barrier. According to the review by Seiler [20] the escape depth is in the range of 0.5 to 1.5 nm for metals, with the transition metals located at the lower end. Not surprisingly, in a direct measurement [27] on Ni(110) a magnetic depth of information of three to four layers (0.4–0.5 nm) was found. A more detailed discussion of the magnetic depth of information, also for inhomogeneous samples, may be found in ref. [13].

Acknowledgements

Our sincere thanks are due to E. Tamura and R. Feder who permitted us to use their results prior to publication.

The hospitality of Professor Ibach at the Institut für Grenzflächenforschung und Vakuumphysik, KFA Jülich is gratefully acknowledged by K. Koike. J. Kirschner owes sincere thanks to Professor T. Ichinokawa and Waseda University, Tokyo, where a part of this work was carried out, for generous hospitality and useful discussions.

References

[1] G. Chrobok and M. Hofmann, Phys. Lett. A 57 (1976) 257.
[2] K. Koike and K. Hayakawa, Jpn. J. Appl. Phys. 23 (1984) L187.
[3] J. Unguris, G.G. Hembree, R.J. Celotta and D.T. Pierce, J. Magn. Magn. Mater. 54–57 (1986) 1629.
[4] J. Kirschner and H.P. Oepen, Phys. Bl. 44 (1988) 227; H.P. Oepen and J. Kirschner, Phys. Rev. Lett. 62 (1989) 819; Scanning Microsc. 5 (1991) 1.
[5] M.R. Scheinfein, J. Unguris, J.L. Blue, K.J. Coakley, D.T. Pierce and R.J. Celotta, Phys. Rev. B 43 (1991) 3395;
M.R. Scheinfein and J.L. Blue, J. Appl. Phys. 69 (1991) 7740.
[6] J. Unguris, D.T. Pierce, A. Galejs and R.J. Celotta, Phys. Rev. Lett. 49 (1982) 72.
[7] H. Hopster, Phys. Rev. B 36 (1987) 2325.
[8] D. Mauri, R. Allenspach and M. Landolt, J. Appl. Phys. 58 (1985) 906.
[9] K. Koike and K. Hayakawa, Jpn. J. Appl. Phys. 23 (1984) L85.
[10] H. Hopster, R. Raue, E. Kisker, G. Güntherodt and M. Campagna, Phys. Rev. Lett. 50 (1983) 70.
[11] E. Kisker, W. Gudat and K. Schröder, Solid State Commun. 44 (1982) 591.
[12] R. Allenspach and M. Landolt, Surf. Sci. 171 (1986) L479.
[13] J. Kirschner, in: Surface and Interface Characterization by Electron Optical Methods, Eds. A. Howie and V. Valdré (Plenum, New York, 1988) p. 267.

[14] J. Kirschner, Phys. Rev. Lett. 55 (1985) 973;
D. Venus and J. Kirschner, Phys. Rev. B 37 (1988) 2199.
[15] J. Kirschner, Surf. Sci. 138 (1984) 191.
[16] We are indebted to Dr. Viefhaus of the Max-Planck-Institut für Eisenforschung, Düsseldorf, for the careful pre-cleaning of the sample, which removed the bulk of the carbon and sulfur impurities.
[17] J. Kirschner, Polarized Electrons at Surfaces, Vol. 106 of Springer Tracts in Modern Physics (Springer, Berlin, 1985).
[18] J. Kirschner and S. Suga, Solid State Commun. 64 (1987) 997.
[19] E. Tamura and R. Feder, Phys. Rev. Lett. 57 (1986) 759.
[20] H. Seiler, J. Appl. Phys. 54 (1983) R1.
[21] O. Paul, M. Taborelli and M. Landolt, Surf. Sci. 221/212 (1989) 724.
[22] M. Taborelli, PhD Thesis, Zürich, 1988, no. ETH-Diss. 8545, unpublished.
[23] R. Feder and J.B. Pendry, Solid State Commun. 26 (1978) 519.
[24] J. Schäfer, R. Schoppe, J. Hölzl and R. Feder, Surf. Sci. 107 (1981) 290.
[25] K.K. Kleinherbers, A. Goldmann, E. Tamura and R. Feder, Solid State Commun. 49 (1984) 735.
[26] R. Feder, B. Awe and E. Tamura, Surf. Sci. 157 (1985) 183.
[27] D.L. Abraham and H. Hopster, Phys. Rev. Lett. 58 (1987) 1352.
[28] P.W. Palmberg, J. Appl. Phys. 38 (1967) 2137.
[29] J. Glazer and E. Tosatti, Solid State Commun. 52 (1984) 905.
[30] D.L. Abraham and H. Hopster, Phys. Rev. Lett. 59 (1987) 2333.
[31] D.R. Penn, Phys. Rev. B 35 (1987) 482.
[32] D.R. Penn, S.P. Apell and S.M. Girvin, Phys. Rev. Lett. 55 (1985) 518.
[33] D.P. Pappas, K.P. Kämper, B.P. Miller, H. Hopster, D.E. Fowler, C.R. Brundle, A.C. Luntz and Z.X. Shen, Phys. Rev. Lett. 66 (1991) 504.
[34] M.P. Gokhale and D.L. Mills, Phys. Rev. Lett. 66 (1991) 2251.
[35] G.A. Mulhollan, Xia Zhang, F.B. Dunning and G.K. Walters, Phys. Rev. B 41 (1990) 8122.
[36] E. Tamura and R. Feder, to be published.
[37] R. Allenspach, M. Taborelli and M. Landolt, Phys. Rev. Lett. 55 (1985) 2599.
[38] M. Landolt, Appl. Phys. A 41 (1986) 83.
[39] R. Allenspach, M. Taborelli, M. Landolt and H.C. Siegmann, Phys. Rev. Lett. 56 (1986) 953.
[40] M. Taborelli, R. Allenspach, G. Boffa and M. Landolt, Phys. Rev. Lett. 56 (1986) 2869.